Supporting Information for "Arctic Ocean response to Greenland Sea wind anomalies in a suite of model simulations"

Morven Muilwijk[1,2], Mehmet Ilicak[3], Sam B. Cornish[4], Sergey Danilov[5], Renske Gelderloos[6], Rüdiger Gerdes[5], Verena Haid[7], Thomas W. N. Haine[6], Helen L. Johnson[4], Yavor Kostov[8], Tamás Kovács[5], Camille Lique[7], Juliana M. Marson[9], Paul G. Myers[9], Jeffery Scott[10], Lars H. Smedsrud[1,2,11], Claude Talandier[7], Qiang Wang[5]

[1]Geophysical Institute, University of Bergen, Bergen, Norway.

[2]Bjerknes Centre for Climate Research, Bergen, Norway

[3]Eurasia Institute of Earth Sciences, Istanbul Technical University, Istanbul, Turkey

[4]Department of Earth Sciences, University of Oxford, Oxford, UK

[5]Alfred-Wegener-Institut Helmholtz-Zentrum für Polar- und Meeresforschung, Bremerhaven, Germany

[6]Department of Earth and Planetary Sciences, The Johns Hopkins University, Baltimore, USA

[7]Laboratoire d'Océanographie Physique et Spatiale, Univ. Brest, CNRS, IRD, Ifremer, IUEM, Brest, France

[8]Department of Physics, University of Oxford, Oxford, UK

[9]Department of Earth and Atmospheric Sciences, University of Alberta, Edmonton, Alberta, Canada

[10]Department of Earth, Atmospheric and Planetary Sciences, Massachusetts Institute of Technology, Cambridge, USA

[11]University Centre in Svalbard, Longyearbyen, Svalbard

Contents of this file

1. Figures S1 to S13

Additional Supporting Information (Files uploaded separately)

1. Captions for Movies S14 to S19

Movie S14.

Vertically integrated concentration of passive tracer released continuously at all depths in the BSO from the ITU model. Panels on the left show the control simulations, middle panels show anomalies resulting from the GSP experiment (stronger wind forcing), and right panels show anomalies resulting from the GSM experiment (weaker wind forcing). Tracer release started simultaneously with the beginning of the perturbation. Values here are not standardized by depth and represent Atlantic Water volume.

Movie S15.

Vertically integrated concentration of passive tracer released continuously at all depths in the BSO from the ITU model. Panels on the left show the control simulations, middle panels show anomalies resulting from the GSP experiment (stronger wind forcing), and right panels show anomalies resulting from the GSM experiment (weaker wind forcing). Tracer release started simultaneously with the beginning of the perturbation. All values are standardized by depth, meaning it represents a percentage of the water column consisting of Atlantic Water from the BSO.

Movie S16.

Vertically integrated concentration of passive tracer released continuously at all depths in the BSO from the MIT model. Panels on the left show the control simulations, middle

panels show anomalies resulting from the GSP experiment (stronger wind forcing), and right panels show anomalies resulting from the GSM experiment (weaker wind forcing). Tracer release started simultaneously with the beginning of the perturbation. Values here are not standardized by depth and represent Atlantic Water volume.

Movie S17.

Vertically integrated concentration of passive tracer released continuously at all depths in the BSO from the MIT model. Panels on the left show the control simulations, middle panels show anomalies resulting from the GSP experiment (stronger wind forcing), and right panels show anomalies resulting from the GSM experiment (weaker wind forcing). Tracer release started simultaneously with the beginning of the perturbation. All values are standardized by depth, meaning it represents a percentage of the water column consisting of Atlantic Water from the BSO.

Movie S18.

Vertically integrated concentration of passive tracer released continuously at all depths in the BSO from the NorESM model. Panels on the left show the control simulations, middle panels show anomalies resulting from the GSP experiment (stronger wind forcing), and right panels show anomalies resulting from the GSM experiment (weaker wind forcing). Tracer release started simultaneously with the beginning of the perturbation. Values here are not standardized by depth and represent Atlantic Water volume.

Movie S19.

Vertically integrated concentration of passive tracer released continuously at all depths in the BSO from the NorESM model. Panels on the left show the control simulations,

middle panels show anomalies resulting from the GSP experiment (stronger wind forcing), and right panels show anomalies resulting from the GSM experiment (weaker wind forcing). Tracer release started simultaneously with the beginning of the perturbation. All values are standardized by depth, meaning it represents a percentage of the water column consisting of Atlantic Water from the BSO.

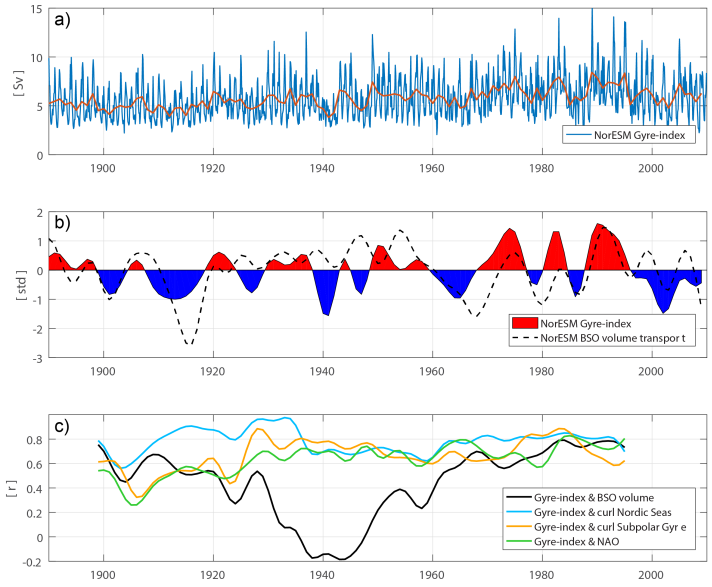

Figure S1. Circulation in the Nordic Seas and related forcing over the last century. a) The mean barotropic streamfunction strength ("Gyre-index") from the forced NorESM 130 year control simulation. Blue line shows monthly values and the red line shows the annual mean. b) Low-pass filtered anomalies of the annual mean barotropic streamfunction (as above) expressed in standard deviations (red and blue) compared with anomalies of annual mean Atlantic Water inflow volume transport through the Barents Sea Opening (BSO, positive north-eastward). Positive values show years with a strong cyclonic barotropic circulation regime and negative values show weak cyclonic circulation . c) Gliding 30-year correlations of the "Gyre-index" anomalies and NAO-index, BSO inflow volume transport, mean wind stress curl strength in the Nordic Seas, and mean wind stress curl strength in the Subpolar Gyre. NAO=North Atlantic Oscillation.

Figure S2. Model mean states from the start of simulation. Note that the Alberta model is simulated over a different period as the others. The JHU model has no variability since it is forced with repeated 1998 forcing.

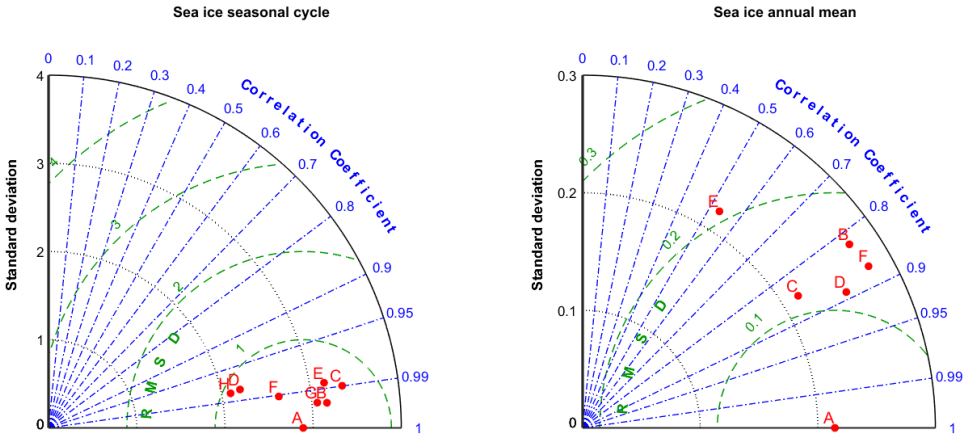

Figure S3. Taylor diagram of the Northern Hemisphere sea ice cover variability from different model control simulations (B=ITU, C=MITB500, D=IFREMER, E=NorESM, F=FESOM, G=JHU and H=Alberta) compared to NSIDC satellite observations (A). Values that appear closest to the (A) in the Taylor diagram are closest to the observations. The JHU model is not included in the right panel because it utilizes a repeat year forcing and hence has no realistic interannual variability. The Alberta model is also not included in the right panel because it covers a different time period.

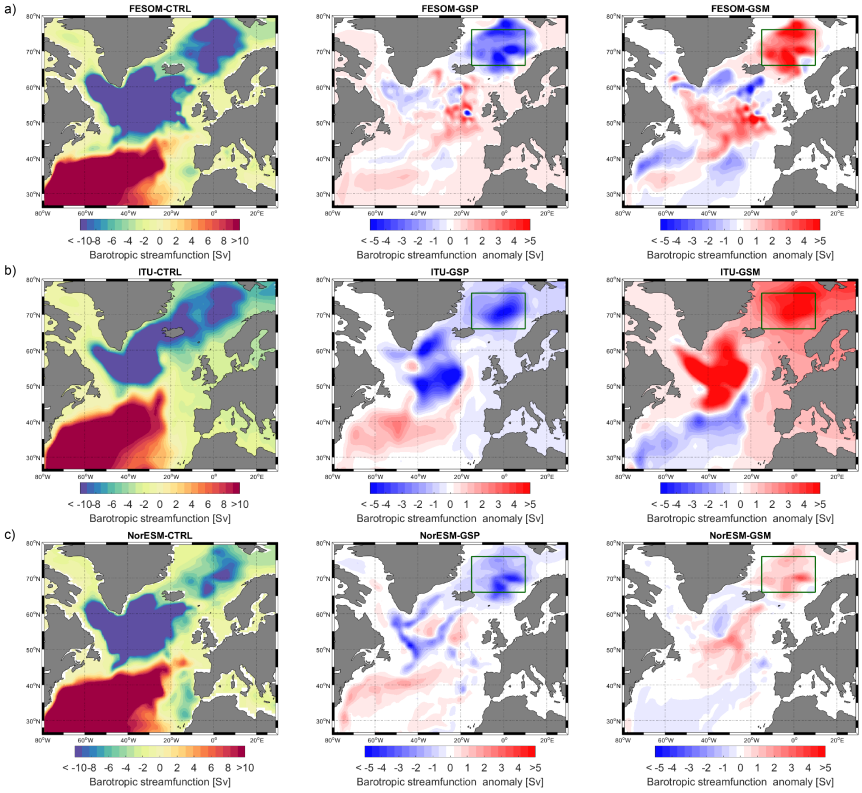

Figure S4. The annual mean response to a 4mb surface pressure anomaly on the barotropic streamfunction in the subpolar gyre region computed from three of the global CRF-models. Negative values denote cyclonic circulation and positive values denote anti-cyclonic circulation. Panels on the left show the control simulations, middle panels show anomalies resulting from the GSP experiment (stronger wind forcing), and right panels show anomalies resulting from the GSM experiment (weaker wind forcing).

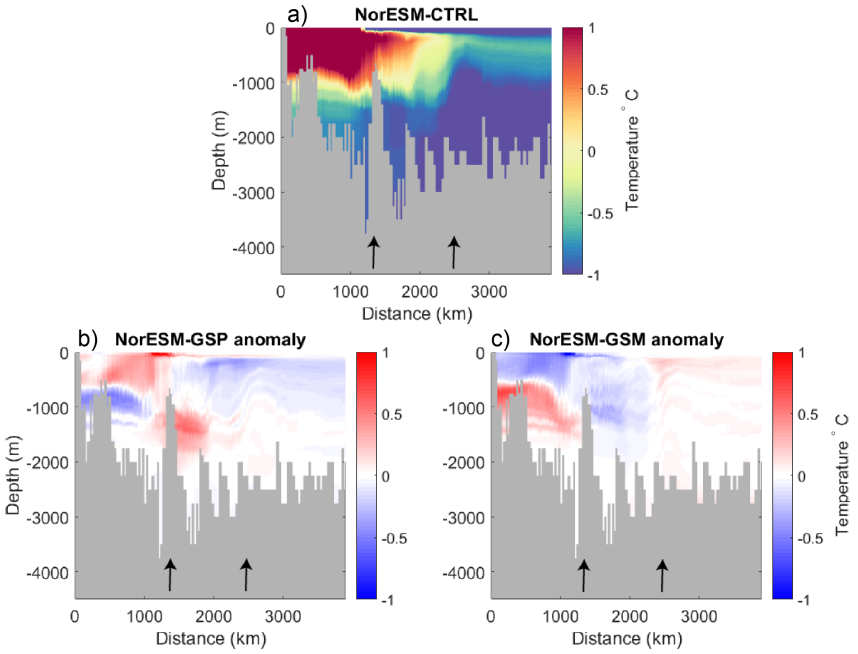

Figure S5. Vertical section of the mean temperature field along the Atlantic Water inflow path for NorESM (section S1 shown in Figure 1). Upper figure shows the mean values, lower figures anomalies resulting from the GSP and GSM experiments. The left arrow in all panels shows Fram Strait while the right arrow shows the St. Anna Trough where water from the Barents Sea exits into the Arctic Basin.

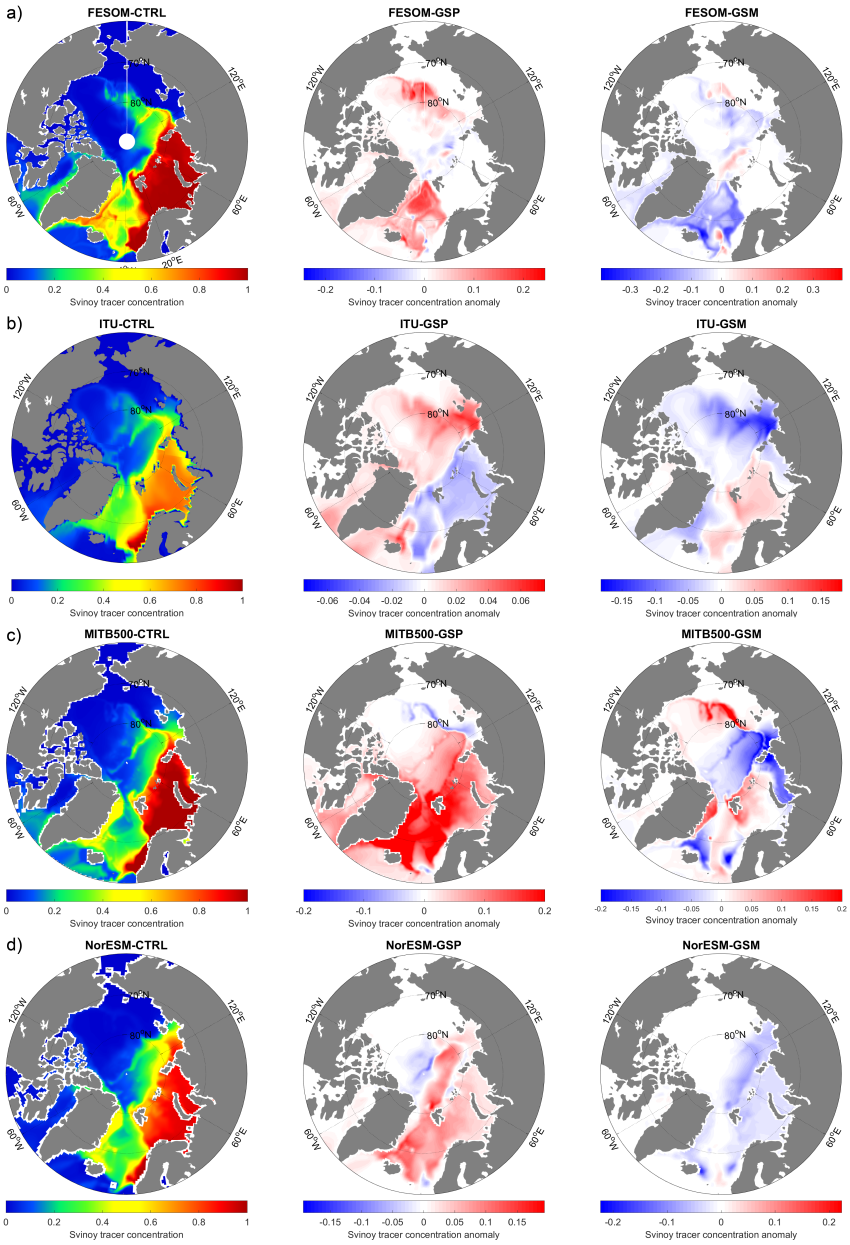

Figure S6. Vertically integrated volume of passive tracer released continuously at all depths at Svinøy in four models. Panels on the left show the control simulations, middle panels show anomalies resulting from the GSP experiment (stronger wind forcing), and right panels show anomalies resulting from the GSM experiment (weaker wind forcing). All values are averaged over model years 20-25. Tracer release started simultaneously with the perturbation start. All values are standardized by depth.

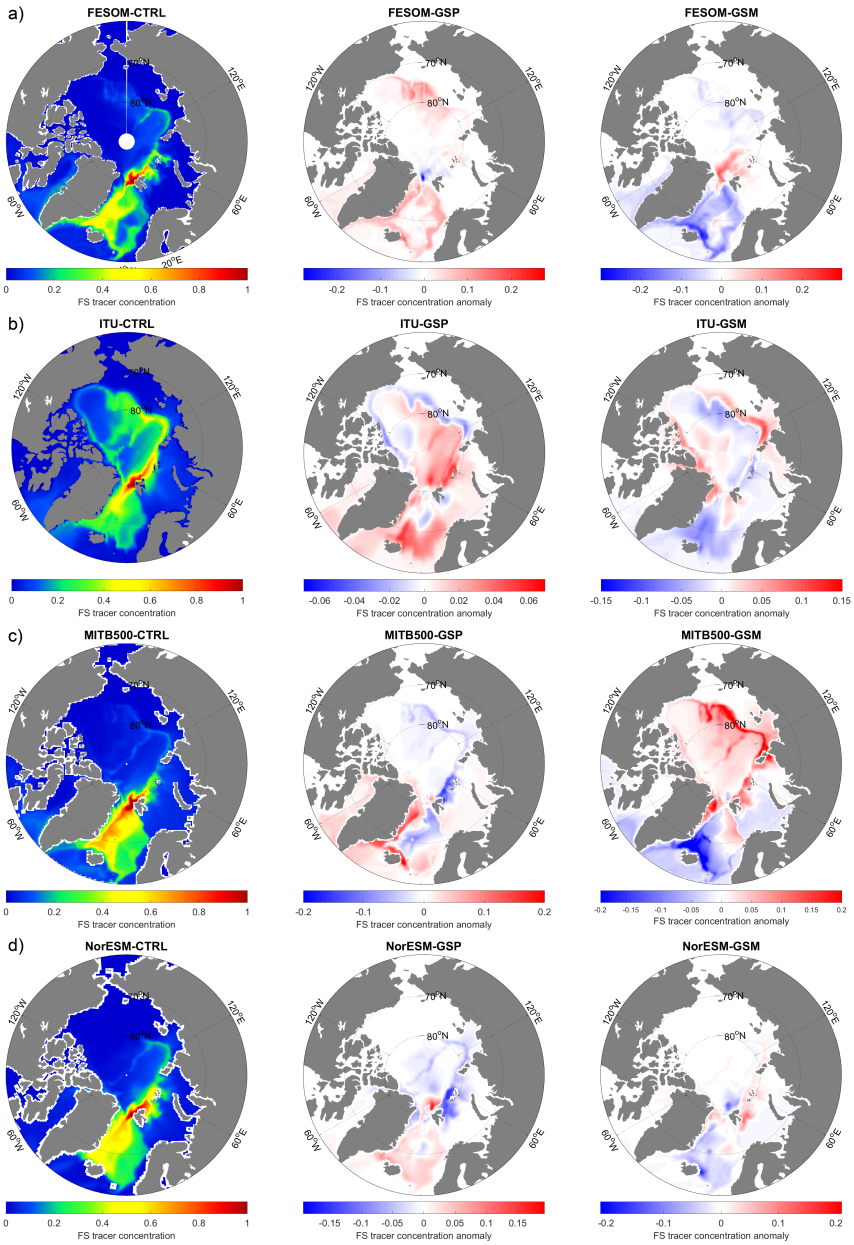

Figure S7. Vertically integrated volume of passive tracer released continuously at all depths in the Fram Strait in four models. Panels on the left show the control simulations, middle panels show anomalies resulting from the GSP experiment (stronger wind forcing), and right panels show anomalies resulting from the GSM experiment (weaker wind forcing). All values are averaged over model years 20-25. Tracer release started simultaneously with the perturbation start. All values are standardized by depth.

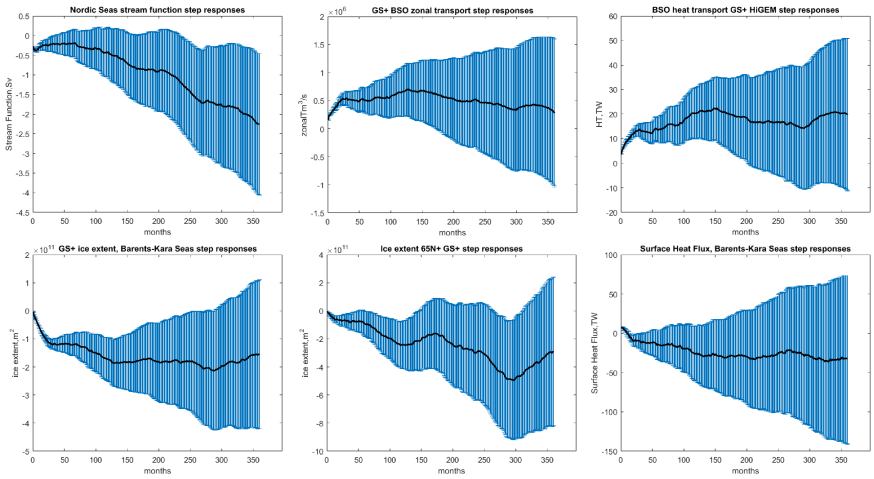

Figure S8. Mean CRF estimates with error bars that arise from the multiple linear regression method used to calculate CRFs from the fully coupled Ox-HiGEM simulation. The estimate of uncertainty is derived from combining, in quadrature, the standard deviation of all estimates with a measure of the error associated with the fit between the original target and a convolution of each impulse estimate and the forcing.

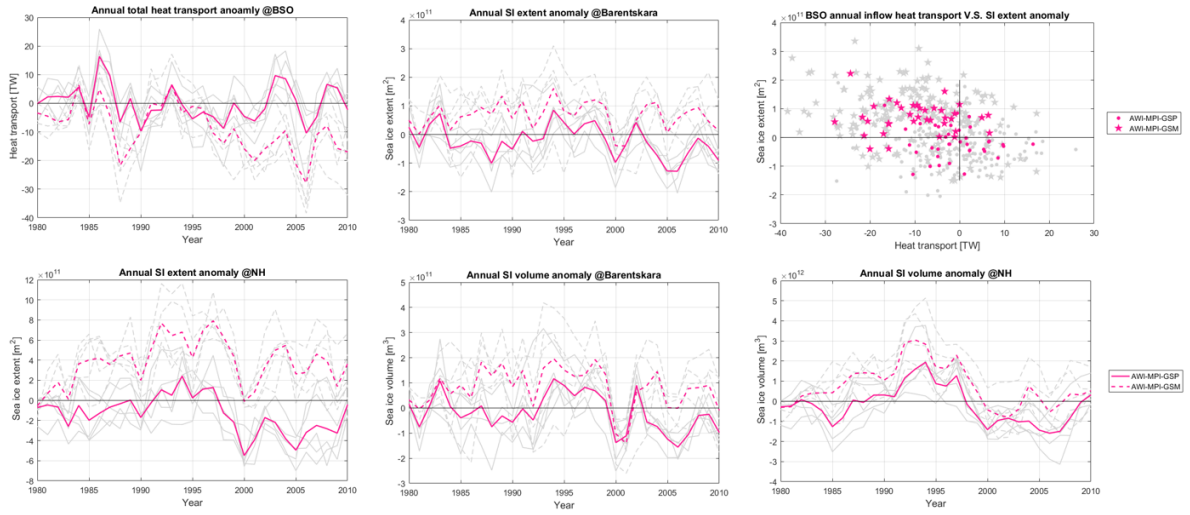

Figure S9. Key Climate Response Functions (CRFs) for the GSP and GSM wind anomalies from the partial coupled AWI-MPI simulations. These CRFs have not been included in the main manuscript (Figure 4 and Figure 6) because no clear response can be identified here. Grey lines represent CRFs from six different ensembles, and the pink lines show the ensemble mean CRFs response. Solid lines represent the response to GSP and dashed lines represent the response to GSM.

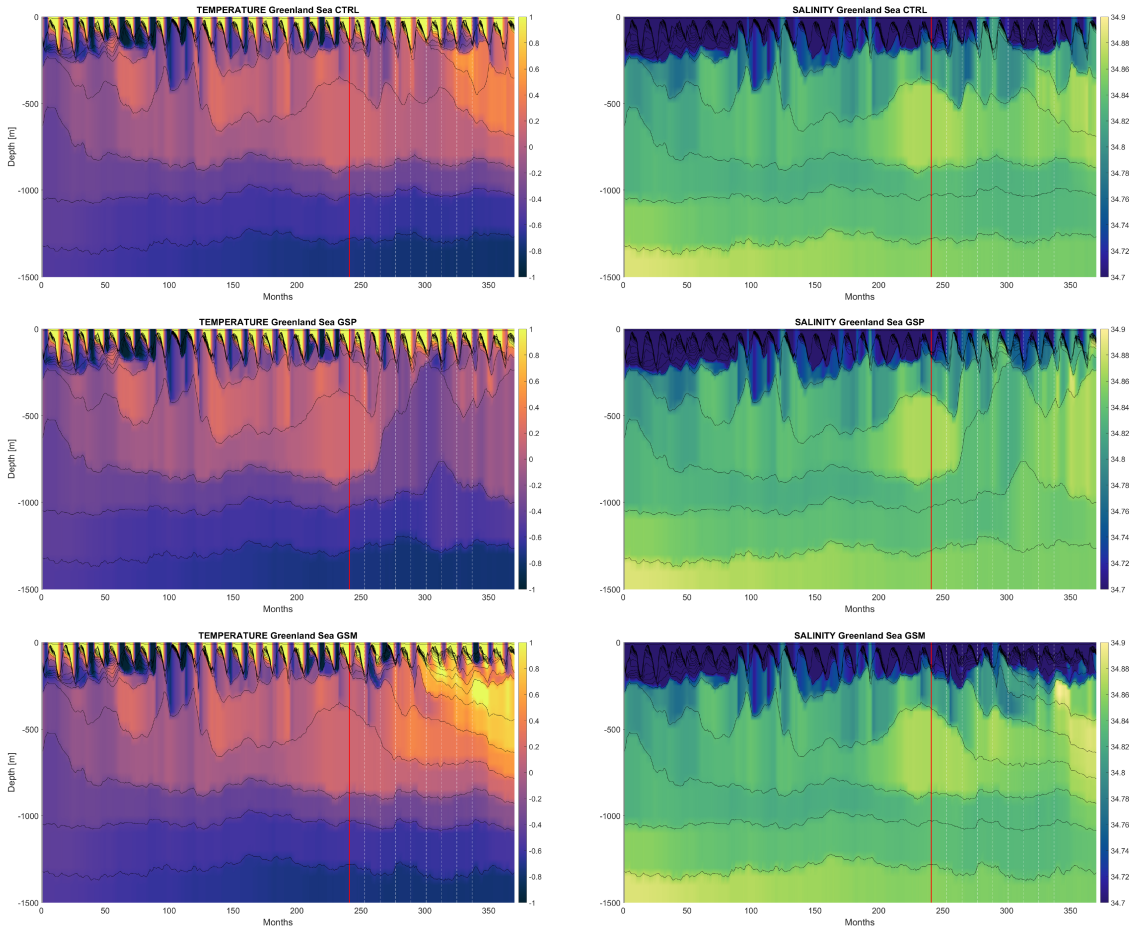

Figure S10. Time evolution of the density field in the central GS before and after the GSP and GSM experiments from the NorESM simulations. Color shading in the left panels shows the temperature by depth for each month, and on the right panels it shows the salinity by depth. Black contours mark different isopycnal layers. Top panels represent the control simulation, middle panels represent the GSP experiment, and lower panels represent the GSM experiment. The red line marks the start of wind perturbation (1980), and dashed white lines each mark one year after the perturbation is applied.

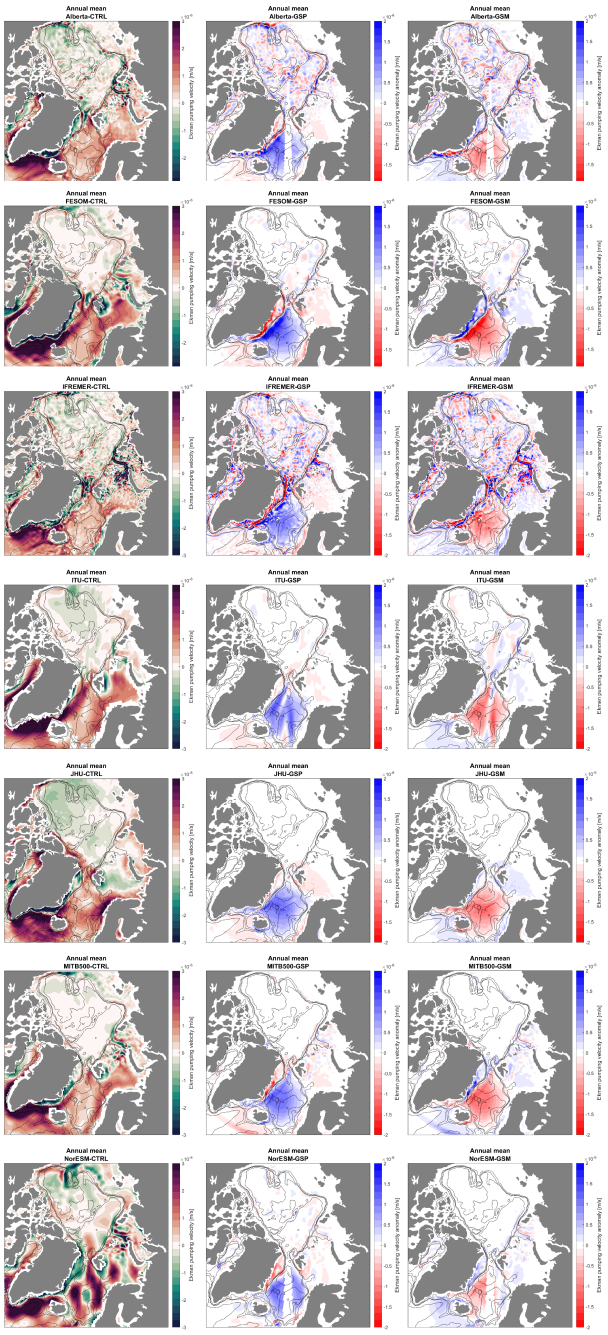

Figure S11. Maps of the annual mean Ekman pumping ($\nabla \times \tau_s/\rho_0 f$) fields computed from the model control simulations and anomalies due to the GSP and GSM experiments. Positive values denote upward velocities. All values are averaged over model years 20-25. Black lines show f/H-contours. For NorESM the EP has been set to zero along the zero meridian. This is due to a small discontinuity in the wind anomaly field, which influences the interpolation plotting tool.

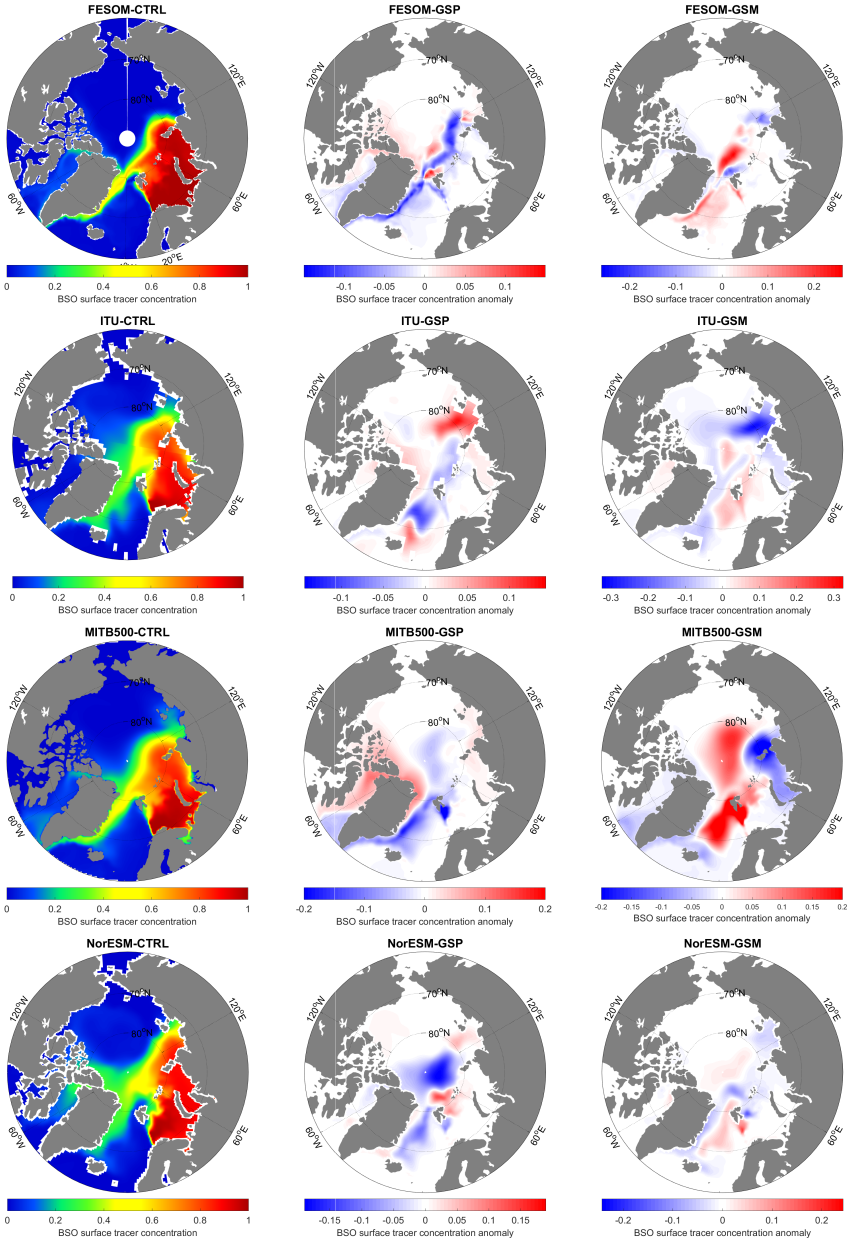

Figure S12. Surface concentration of passive tracer released continuously in the BSO in four models. Panels on the left show the control simulations, middle panels show anomalies resulting from the GSP experiment (stronger wind forcing), and right panels show anomalies resulting from the GSM experiment (weaker wind forcing). All values are averaged over model years 20-25. Tracer release started simultaneously with the perturbation start.

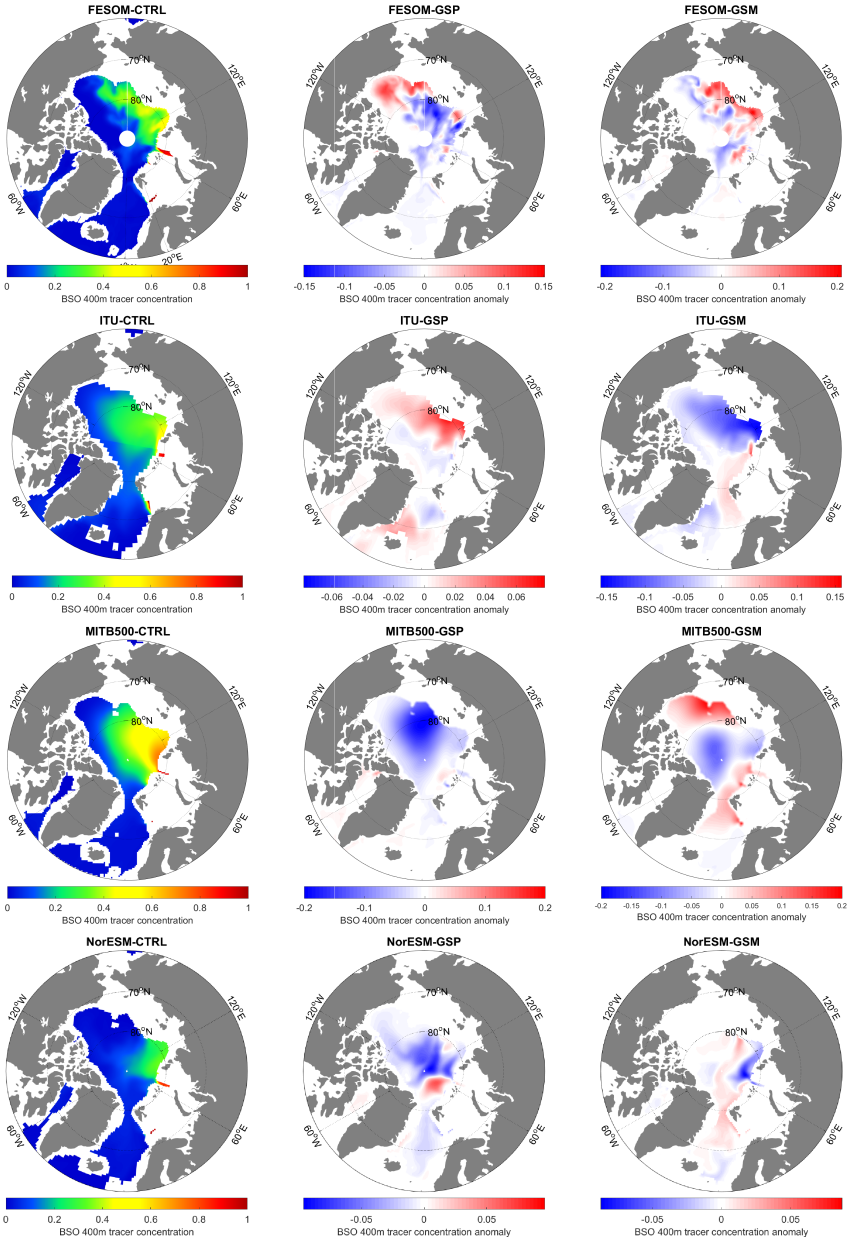

Figure S13. Concentration of passive tracer released continuously in the BSO in four models at intermediate depth (400 m). Panels on the left show the control simulations, middle panels show anomalies resulting from the GSP experiment (stronger wind forcing), and right panels show anomalies resulting from the GSM experiment (weaker wind forcing). All values are averaged over model years 20-25. Tracer release started simultaneously with the perturbation start.